

# Influence of porosity and pore fluid on acoustic properties of chalk: AVO response from oil, South Arne Field, North Sea

Peter Japsen<sup>1</sup>, Anders Bruun<sup>2</sup>, Ida L. Fabricius<sup>3</sup>, Rasmus Rasmussen<sup>1</sup>, Ole V. Vejbæk<sup>1</sup>,  
Jacob Mørch Pedersen<sup>2</sup>, Gary Mavko<sup>4</sup>, Christian Mogensen<sup>2, 5</sup> and Christian Høier<sup>1,6</sup>

<sup>1</sup> Geological Survey of Denmark and Greenland (GEUS), DK-1350 Copenhagen K, Denmark (e-mail: pj@geus.dk)

<sup>2</sup> Ødegaard A/S, DK-2200 København N, Denmark

<sup>3</sup> Technical University of Denmark (DTU), DK-2800 Lyngby, Denmark

<sup>4</sup> Stanford University, California 94305-2215, USA

<sup>5</sup> Present address: Denerco Oil, DK-2840 Holte, Denmark

<sup>6</sup> Present address: Dong A/S, DK-2970 Hørsholm, Denmark

**ABSTRACT:** Amplitude versus offset (AVO) inversion provides direct evidence for the presence of light oil in high-porous chalk in the South Arne Field, North Sea. The elastic properties of the chalk were estimated at three scales by analysing core data, log-readings and AVO-inversion results. The velocity–porosity relation of the core data matches a modified upper Hashin–Shtrikman model for Ekofisk Field chalk and the model is extended to 45% porosity. A small clay content reduces porosity without affecting chalk stiffness and this content can be estimated from the water saturation, which is controlled by silicate content and particle sorting in the zone of irreducible water saturation. The model is, thus, scaled according to clay content estimated by the water saturation. Based on comparison with the model and measurements on core samples, it is found that the sonic log data represent chalk characterized by forced displacement of the oil by mud filtrate and, thus, a much higher water saturation than estimated from, for example, a shallow resistivity log. Forward modelling of the acoustic properties of the virgin zone results in a characteristic pattern of Poisson ratio versus depth. This pattern agrees with inverted seismic data, whereas it is not captured by conventional fluid substitution.

**KEYWORDS:** *acoustic properties, chalk, fluids, North Sea, porosity*

## INTRODUCTION

Understanding the influence of pore fluids on acoustic properties of sediments is a central issue for evaluating seismic data; e.g. in amplitude versus offset (AVO) techniques that depend on the discrimination of fluid content from variations in P- and S-velocities (e.g. Castagna & Backus 1993). Much research has been focused on describing such effects in sandstone, whereas studies on the rock physics of chalk have appeared mainly in recent years (e.g. Walls *et al.* 1998; Japsen *et al.* 2000; Fabricius *et al.* 2002; Gommesen *et al.* 2002; Røgen 2002; Fabricius 2003; Gommesen 2003; Vejbæk *et al.* 2005; Røgen *et al.* in press). In the North Sea, chalk is an important reservoir rock and more information could be extracted from seismic data if the fundamental physical properties of chalk were understood better. A phase-reversal due to the presence of gas in chalk was documented by Megson (1992), but, so far, the presence of oil in chalk has not been demonstrated to have an effect on surface seismic data. The need for a better link between chalk reservoir parameters and geophysical observations has only increased since the discovery of the Halfdan Field proved major reserves outside four-way dip closures (Jacobsen *et al.* 1999; Vejbæk & Kristensen 2000).

We have investigated the acoustic properties of the chalk of the Danian Ekofisk Formation and the Maastrichtian Tor

Formation in the Danish South Arne Field, where porosities up to 45% are found in the Tor reservoir at almost 3 km depth (Fig. 1; Mackertich & Goulding 1999). Important factors for the preservation of porosity are early hydrocarbon migration and overpressure of *c.* 15 MPa caused by compaction disequilibrium (e.g. Scholle 1977; Japsen 1998). Based on ultrasonic measurements, we found that for porosities above *c.* 30%, there is a pronounced change in the relation between P- and S-velocities for chalk saturated with light oil. This change makes it probable that the light oil in the high-porous chalk of the South Arne Field may be detected through AVO inversion of surface seismic data. But the link between the surface seismic data and the reservoir is hampered by invasion of mud filtrate into the zone where the sonic log is registered (cf. Gommesen *et al.* 2002). We found that the acoustic properties of the reservoir agree with those estimated from AVO inversion if they are computed from a modified upper Hashin–Shtrikman model, as suggested by Walls *et al.* (1998), with porosity and water saturation of the virgin zone as input.

## DATA

### Measurements on core plugs

Ultrasonic measurements (700 kHz) were carried out on 34 chalk samples of the Ekofisk and Tor formations from the

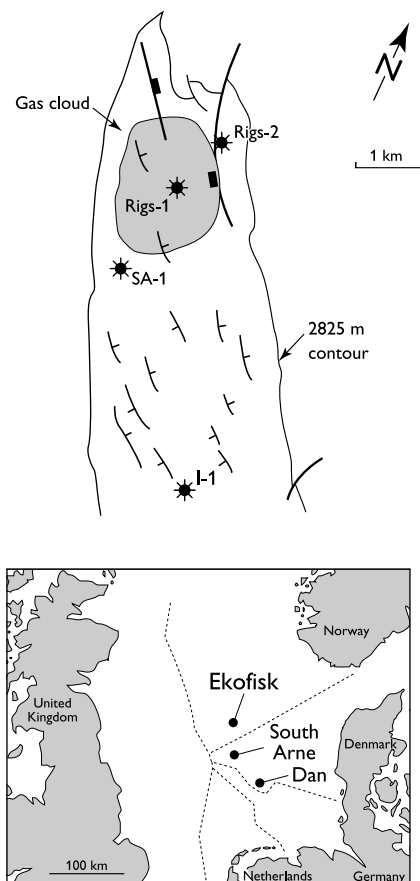


**Fig. 1.** The South Arne Field, top chalk structure. Location of wells and gas cloud above the chalk from seismic sections. Modified after Mackertich & Goulding (1999).

South Arne Field under both dry and fully saturated conditions; wells SA-1, Rigs-1 and Rigs-2 (Fig. 2; see also Røgen *et al.* in press; Japsen *et al.* 2002). In order to prevent over-dry conditions, the samples were kept at room moisture for two months after being dried at 110 °C. During this procedure three samples with high clay content regained high water content after drying, probably due to re-hydration of the smectite (water saturation,  $S_w=7\text{--}12\%$ ; kaolinite plus smectite content 3–12%). The water saturation in the saturated plugs was generally between 97% and 103% (related to minor weight and saturation errors), but low permeability prevented total saturation in three samples ( $S_w=92\text{--}95\%$ ). Compressional and shear wave velocities,  $V_p$  and  $V_s$  [ $\text{km s}^{-1}$ ], were determined from measured sample lengths and readings of travel times. The ultrasonic velocities were measured at 75 bar hydrostatic confining pressure and the results showed only minor influence of pressure changes. The results were corrected to 0% and 100% saturation (see the ‘Results’ section).

Density,  $\rho$  [ $\text{g cm}^{-3}$ ], grain density,  $\rho_{gr}$ , porosity,  $\phi$  [fractions] and permeability,  $k$  [Darcy] were also determined. Mineralogical composition of the samples was estimated on the basis of X-ray diffraction data, backscatter electron microscopy of epoxy-impregnated polished samples. Carbonate titration indicated that the Tor Formation samples contain 92–100% calcite (Røgen *et al.* in press), samples from the Ekofisk Formation contained 59–91% calcite.

Good correlation is observed between P- and S-velocity and porosity for dry and saturated samples (Fig. 2). Three samples with high clay content have outlying values relative to these trends. The low velocities of these samples compared to their

porosity indicate that the clay is occupying pore space, thus, reducing porosity, but the relatively high Poisson ratio of these samples suggests that the clay also have some effect on the load-bearing matrix.

### Log data

Well log data for the chalk in six wells in the South Arne Field were quality controlled. Four of the wells have readings of  $V_p$  and  $V_s$  and, of these wells, data were selected for the near-vertical Rigs-2 well for further analysis because good core data are available for this well and because it is situated outside the ‘gas cloud’ seen in the chalk overburden on seismic sections across the South Arne Field (Fig. 1). Porosity was estimated from log readings of the bulk density,  $\rho_{bulk}$ , assuming full invasion of the mud filtrate and, thus, density was converted to porosity based on mud filtrate densities rather than of mixtures of brine and hydrocarbons ( $\rho_{mud}=1.03 \text{ g cm}^{-3}$ ;  $K_{mud}=3.12 \text{ GPa}$ ). Furthermore, water-based mud was used in this well. These estimates of porosity were found to match porosity measured on core samples from the Rigs-1 and -2 wells (Fig. 3).

Water saturation,  $S_w$  fraction, was estimated for the virgin zone from a range of pore water resistivity values based on the LLS and LLD logs. A shallow resistivity log revealed a large scatter in the determination of the saturation,  $S_{so}$ , in the zone invaded by mud filtrate. The density,  $\rho$ , of chalk for a given water saturation was calculated as a function porosity,  $\phi$ :

$$\rho = \rho_{oil}(1 - S_w)\phi + \rho_{brine} \cdot S_w \cdot \phi + \rho_{matrix}(1 - \phi) \quad (1)$$

for the density of oil, brine and chalk matrix ( $\rho_{oil}$ ,  $\rho_{brine}$ ,  $\rho_{matrix}$ ) in the reservoir of the South Arne Field (Table 1).

Shale volume was calculated from the gamma log, based on a calibration to the measured gamma-ray level in the sealing shale sequence relative to the purest chalk interval in each well. However, the relation between the gamma response and the clay content in the chalk may be rather arbitrary and the presence of, for example, smectite and silica, is not recorded by the gamma log.

### Seismic data

Near- and far-offset data were available from a 3D survey covering the South Arne Field. The two sub-cubes were generated as partial stacks, offset defined. Near- and far-offset data were available from a 3D survey covering the South Arne Field. The two sub-cubes were generated as offset stacks using mute polygons.

## RESULTS

### Ultrasonic measurements during drainage

Two chalk samples were measured during drainage. It was found that extrapolation of the bulk modulus from almost full water saturation to 100% and from almost dry conditions to 0% could be done by calculating the fluid properties as a Voigt average and as a Reuss average, respectively (see equations (A2), (A3) in Appendix A; cf. Figure 4). This indicates that the water is finely mixed in the air at low saturations, whereas the air occurs as patches at high saturation. The data from the laboratory measurements were corrected to 0% and 100% saturation accordingly (Fig. 2). The shear modulus was almost unaffected by the degree of water saturation in the partially saturated plugs, as predicted by Gassmann’s relations (see

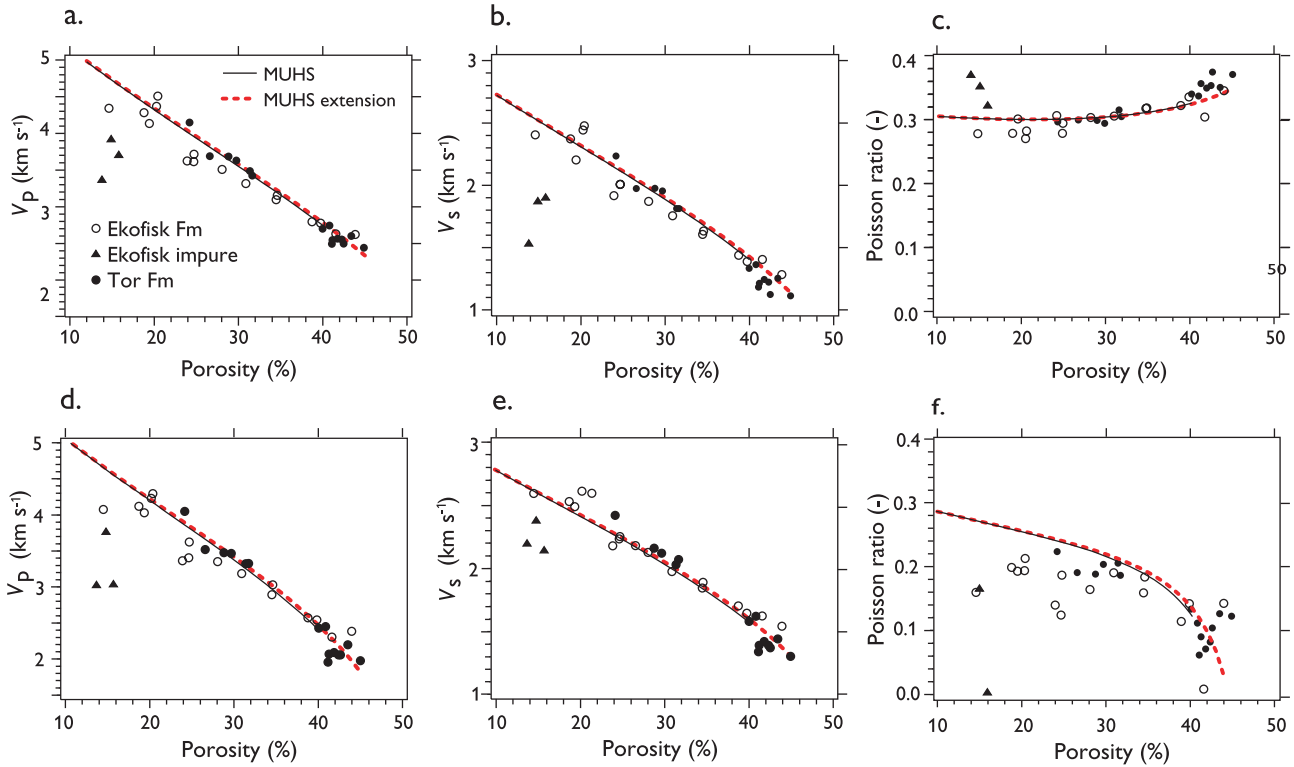


**Fig. 2.** Acoustic properties of 34 chalk samples versus porosity measured at saturated and dry conditions, upper and lower panel. Fluid substitution to 100% saturation at reservoir conditions and to 0% saturation, respectively, (a), (d) P-velocity; (b), (e) S-velocity; (c), (f) Poisson ratio. Good agreement is observed between the South Arne core data and the MUHS model based on log data from the Ekofisk Field (full line; equation (A5); Walls *et al.* 1998). Extrapolation of the model from 40% to 45% porosity, which agrees with the plug data (dashed line; equation (2)) is suggested. One dry sample with high shale content has negative Poisson ratio (f). MUHS, modified upper Hashin–Shtrikman.

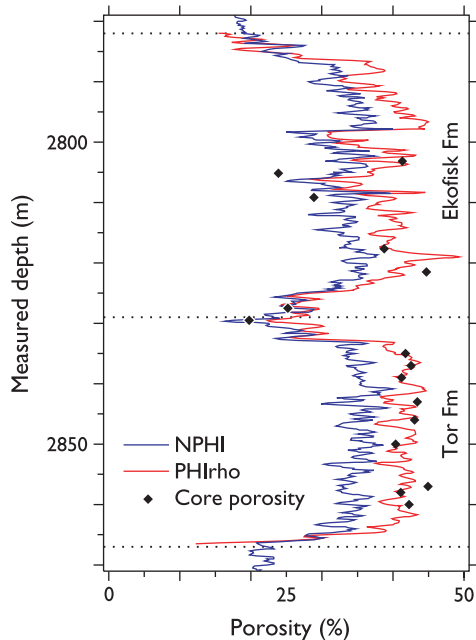


**Fig. 3.** Porosity logs for the Rigs-2 well and data points for core porosity. Note the agreement between core porosity and the density log, PHIrho, which was estimated from log readings of the bulk density,  $\rho_{\text{bulk}}$ , assuming full invasion of the mud filtrate. The neutron porosity log, NPHI, underestimates porosity due to the presence of hydrocarbons.

equation (A1)). However, the shear modulus at 0% saturation was 0.5 GPa higher than at the non-zero saturations for the

**Table 1.** Elastic properties: bulk and shear modulus,  $K$  and  $G$ , and density,  $\rho$

	$K$ (GPa)	$G$ (GPa)	$\rho$ (g cm <sup>-3</sup> )
Calcite	71	30	2.71
Clay	25	9	2.70
Brine	2.96 <sup>a</sup>	0	1.035 <sup>b</sup>
Hydrocarbon	0.52 <sup>a</sup>	0	0.633 <sup>b</sup>

Mineral properties after Mavko *et al.* (1998). Fluid properties estimated for the Rigs-2 well.

<sup>a</sup>Densities estimated at reservoir level at the South Arne Field (J. Jensenius, pers. comm. 2002).

<sup>b</sup>Values for fluids at the crest of the South Arne Field estimated with Batzle–Wang algorithm for  $T=100^\circ\text{C}$ ,  $P=44\text{ MPa}$ , Oil gravity=33 API, Gas gravity=0.815 (A. Colby, pers. comm. 2002). GOR=1685 SCF BBL<sup>-1</sup> in order to match the hydrocarbon density.

samples investigated. This is due to some over-dry effect which has been observed for other rock types as well (see Japsen *et al.* 2002).

### Comparison of log and core data

Porosity,  $V_p$  and  $V_s$  based on log measurements and core data were estimated at the same depths after the log depths had been shifted to match the core depths. This was done by correlating the wellbore Th-log to the core-scanned Th-log for the Rigs-1 and Rigs-2 wells, whereas no depth shift was made for the SA-1 well. The values of  $V_p$ - and  $V_s$ -core were estimated for brine at reservoir conditions and the values of  $V_s$ -core are only expected to be slightly smaller than  $V_s$ -log for full oil saturation because the shear modulus is unaffected by the fluid content.

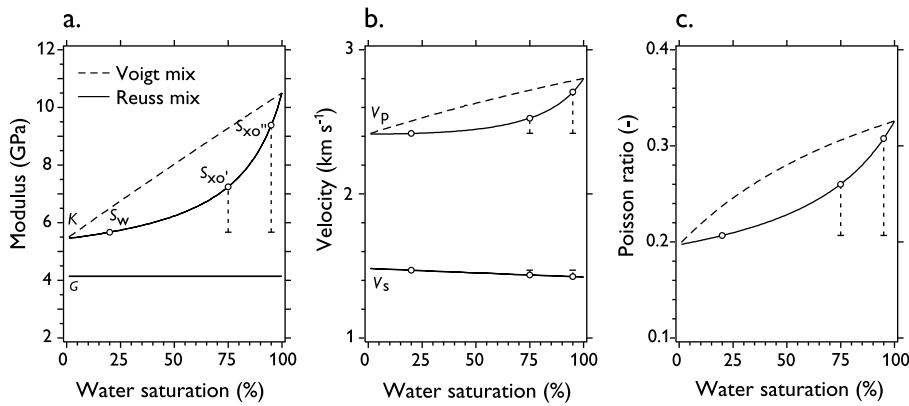


**Fig. 4.** Acoustic properties as a function of water saturation for chalk with 40% porosity. (a) Bulk and shear modulus; (b) P- and S-velocities; (c) Poisson ratio. Flushing of the reservoir increases the bulk modulus of the oil-brine mixture along a Reuss curve (equation (A2)). Minor variations in the estimation of  $S_{xo}$  result in major changes in the acoustic properties (vertical lines). MUHS prediction with fluid properties for the South Arne Field (equation (2); Table 1).  $S_w$ , water saturation of the virgin zone;  $S_{xo}$ , saturation of the mud-invaded reservoir from Land's equation (equation (4));  $S_{xo}''$ , saturation of the mud-invaded reservoir from sonic data (equation (8)).

$V_p$ -core is expected to be much higher than  $V_p$ -log in the oil zone due to the density differences between the saturating fluids.

The correlation is high between porosities estimated from log and core data, but core porosities are generally slightly higher than log porosities at high porosities (Fig. 5a). This could be due to an averaging effect of the log tool.

The correlation between  $V_p$  estimated from log and core data is very high at low velocities and this indicates a very high degree of invasion of mud filtrate in the zone near the wellbore (Figs. 3, 5b). At intermediate velocities ( $V_p \approx 3.5 \text{ km s}^{-1}$ )  $V_p$ -core is higher than  $V_p$ -log whereas  $V_s$ -core is close to  $V_s$ -log and the invasion of mud filtrate is, thus, probably less at intermediate porosities ( $\phi \approx 30\%$ ). At high velocities ( $V_p > 3.75 \text{ km s}^{-1}$ ) both  $V_p$  and  $V_s$  are approximately equally higher for core than for log data and this indicates that the core data sample variations occur over much smaller distances than the log data: the sonic log measures velocities over about 1 m whereas the laboratory measurements are carried out on plug samples about 2 cm long (e.g. the discrepancy between the two datasets at the top Tor velocity peak; Figure 6b). In contrast, both porosity datasets measure changes on a cm-scale.

The correlation between S-velocities estimated from log and core data is good at intermediate values, but core velocities are relatively high for high velocities and relatively low for low velocities (Fig. 5c). This is probably due partly to the different scales of sampling for the two datasets, as described above. However, the core data plot systematically below the shear-wave log in the high-porosity Tor Formation, even though most of these data points have identical porosity estimates for both datasets (Fig. 7b). The reason for this bias could also be related to scaling because the sonic finds 'faster paths' in the earth where it samples the lowest porosities. This is probably important at high porosities because the S-velocities become very low and small changes in velocity reflect large differences in travel times ( $V_s < 1.5 \text{ km s}^{-1}$  for  $\phi > 40\%$ ). Alternatively, the discrepancies could be related to problems measuring slow S-waves in the borehole. However, cross-plots of  $V_p$  versus  $V_s$  for the sonic data reveal a steady relationship with no deviations at low velocities, which could be due to, for example, P-arrivals from the fluid being misinterpreted as S-arrivals.

#### Extended MUHS model based on ultrasonic data

Ultrasonic data from core samples from the South Arne Field are in good agreement with the velocity-porosity modified upper Hashin-Shtrikman ('MUHS') model of Walls *et al.* (1998) for chalk in the Ekofisk Field, based on log data with porosities less than 40% (Fig. 2; equations (A4), (A5)). However, chalk

porosities between 40% and 45% occur on the South Arne Field, whereas low-porosity, pure chalk is not encountered in the wells in this study. For this reason, the range of the MUHS model was extended from 40% to 45% by estimating the high-porosity end-member at 45% porosity, while keeping the low-porosity end-member unchanged (equations (A4), (A5)):

$$K_{\phi_{\max}} = 1.5 \text{ GPa}, G_{\phi_{\max}} = 2.5 \text{ GPa for } \phi_{\max} = 45\% \quad (2)$$

The extended MUHS model can be applied to compute elastic moduli and Poisson's ratio for chalk as a function of porosity for the range of water saturations encountered on the South Arne Field (Table 1), where the Poisson ratio,  $\nu$ , is defined as:

$$\nu = \frac{3K - 2G}{2(3K + G)} = \frac{V_p^2/V_s^2 - 2}{2(V_p^2/V_s^2 - 1)} \quad (3)$$

In Figure 8 we see that even minor amounts of oil shift the bulk modulus down as expected from the assumed fine-scale Reuss mixing of the fluids (equation (A2)). The shear modulus is, however, unaffected by fluid properties as predicted by Gassmann's relations and, consequently, pronounced variations in the Poisson ratio are predicted at high porosities. For pure brine, Poisson's ratio is almost constant  $\approx 0.31$  for  $10\% < \phi < 35\%$ , but increases to 0.35 for  $\phi = 45\%$  (cf. Gommessen 2003). For saturation with pure oil, Poisson's ratio decreases to 0.14 for  $\phi = 45\%$  and there is, thus, a pronounced span in Poisson's ratio for porosities above  $\approx 30\%$  between heavy brine and light oil. This span in Poisson ratio, predicted by the MUHS model, makes it probable that the light oil in the high-porous chalk on the South Arne Field might be detected through AVO inversion of surface seismic data.

#### ACOUSTIC PROPERTIES OF THE VIRGIN ZONE

The acoustic properties of high-porosity chalk depend critically on fluid content (cf. Figure 8). One may expect that the acoustic signal travels in the zone close to the wellbore, where invasion of mud filtrate is likely because the sonic velocity will be highest where the fluid density is highest. The sonic data were examined by comparing them to the MUHS model for brine at reservoir conditions (equation (2); Table 1) and it was found that:

1. the sonic data appear to be influenced by the presence of hydrocarbons (Fig. 9A): Bulk modulus and Poisson's ratio are low compared to the MUHS model, and the high-porosity chalk appears to be almost completely flushed as

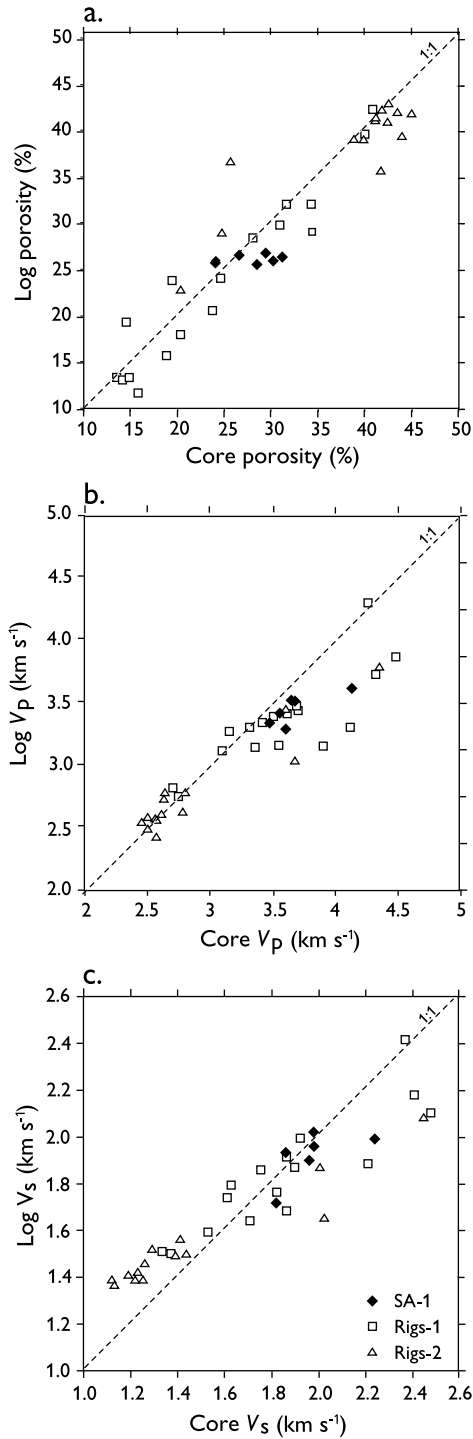


**Fig. 5.** Correlation between log data and data for saturated core samples at identical depths. Fluid substitution to 100% saturation at reservoir conditions for the core data. (a) Porosity; (b) P-velocity; (c) S-velocity. The porosity estimates and intermediate P- and S-velocities are close to 1:1 relations. The 1:1 relation for  $V_p$ -log at low velocities indicates that  $V_p$ -log is measured in a zone with almost full invasion of mud filtrate, whereas the high values of  $V_s$ -log indicate that the shear wave chooses a relatively 'fast path'.

the bulk modulus data are close to the brine-filled model for  $\phi > 40\%$ . The shear modulus (which is unaffected by fluid content according to Gassmann theory) plots close to the MUHS trend for  $30\% < \phi < 40\%$  (see the 'Results' section and below in this section);

2. the sonic data appear to become overcorrected if the data are transformed to brine conditions assuming no invasion of mud filtrate (Fig. 9B): the bulk modulus plots above the MUHS model for high porosities.

It is, therefore, found that the  $V_p$  log in the Rigs-2 well was measured in chalk where oil is present, but in smaller amounts than indicated by  $S_w$  due to invasion of mud filtrate (cf. Gommessen *et al.* 2002).

Two approaches may now be followed to estimate the acoustic properties of the virgin zone so that the well data can be compared with seismic data:

1. Transform the sonic data to  $S_w$ -conditions based on an approximation to the scattered estimate of  $S_{xo}$  from shallow resistivity data (Fig. 6).
2. Estimate the acoustic properties from the MUHS model with  $f\phi$  and  $S_w$  as input. The bulk moduli estimated from the model and from the data may be used to quantify  $S_{xo}$  using Gassmann's relations (Fig. 7).

#### Virgin zone properties estimated from Land's equation

The estimated water saturation close to the wellbore,  $S_{xo}$ , shows a considerable scatter ranging from the saturation in the virgin zone to an upper value given by Land's formula (Land 1968) (Fig. 6):

$$S_{xo} = 1 - \frac{1 - S_{wi}}{1 + C(1 - S_{wir})} \quad (4)$$

where  $S_{wi}$  is the initial water saturation ( $=S_w$ , the saturation of the virgin zone),  $S_{wir}$  is the irreducible water saturation and  $C=2.5$  for the South Arne Field (F. If 2003, pers. comm.).  $S_{wir}$  can be calculated from the normalized capillary pressure curve method developed for the tight chalk in the North Sea (the equivalent radius method, EQR; Engström 1995) :

$$S_{wir} = \left(\frac{A}{\phi}\right)^B \quad (5)$$

where  $A$  and  $B$  are dimensionless constants. For the Rigs-2 well,  $S_{xo}$  is computed based on these two equations, where distinction is made between the Ekofisk and Tor formations and  $S_{wir}$  is higher for the Ekofisk Formation (Fig. 6):  $A=0.12641$ ,  $B=2.45422$  (Ekofisk Fm.) and  $A=0.06596$ ,  $B=2.19565$  (Tor Fm.) (P. Frykman 2003, pers. comm.). The mean water saturation is predicted to increase from 17% to 76% in the flushed zone of the Tor Formation and  $S_{xo}$  is seen to mirror  $S_w$ , so that relatively more oil is removed from the more oil-saturated intervals (Fig. 6a).

The acoustic properties of the invaded zone can, thus, be computed from the velocity logs (blue curves in Figure 6b) and the water saturation  $S_{xo}$  approximated by Land's equation. The properties of the virgin zone (red curves) may be estimated from this dataset by fluid substitution to water saturation, given by  $S_w$ . The P-velocity of the invaded zone and of the virgin zone are not predicted to differ much because the fluid properties are rather identical for medium saturations due to the assumed fine-scale Reuss mixing of the fluids (Fig. 4). A bigger change in  $V_p$  is predicted from the data curve to the brine curve (green). This is to be expected because minor amounts of light fluids reduce the bulk modulus of the brine greatly.

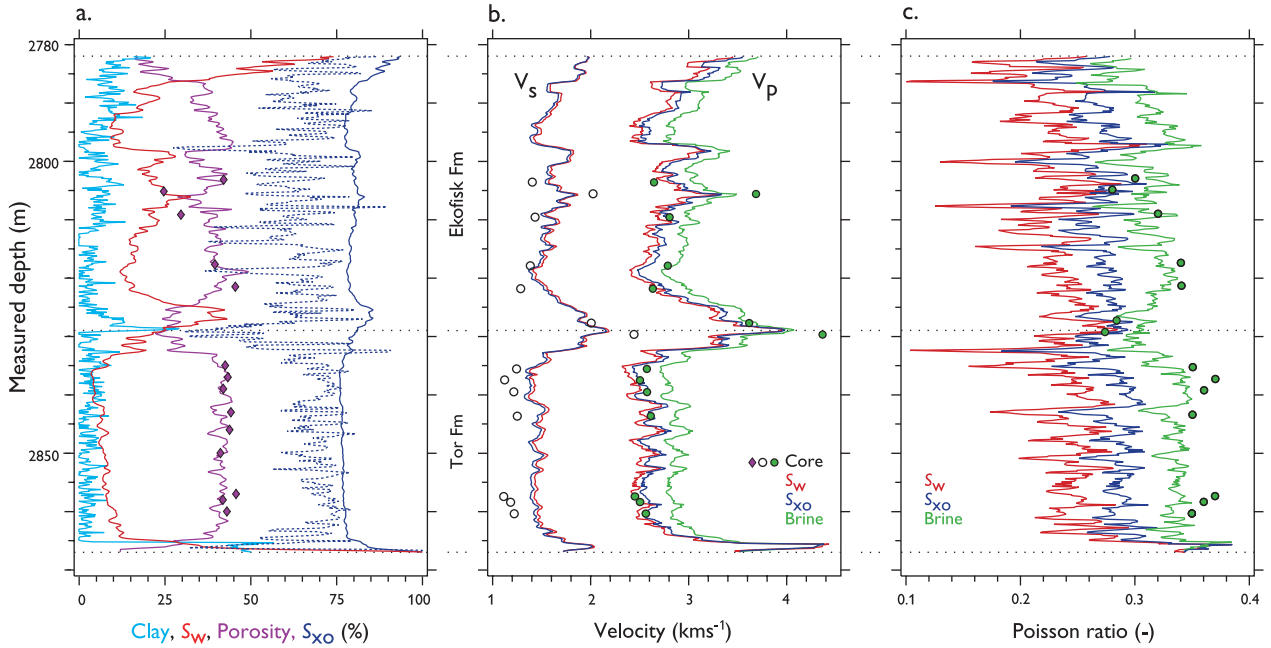


**Fig. 6.** Log data and predictions based on Land's (1968) estimate of residual oil for the chalk section in the Rigs-2 well (equation (4)). (a) Clay content (from gamma log), porosity and water saturation,  $S_w$  and  $S_{XO}$  from Land's equation (full line; equation (4)) and from the shallow resistivity log (dashed line); (b) P- and S-velocity. Data and predictions. Brine-estimate for  $V_s$  not shown; (c) Poisson ratio. Data and predictions. In the high-porosity oil zone of the Tor Formation,  $S_{XO}$  is predicted to be  $\approx 75\%$ . Due to the Reuss mixing of the fluids the acoustic properties of the invaded and virgin zones do not differ much. This is indicated by the closeness of the measured  $V_p(S_{XO})$  (blue curve) and the predicted  $V_p$ (virgin zone) (red curve), whereas  $V_p$ (brine) (green curve) is predicted to be significantly higher (cf. Figure 4).

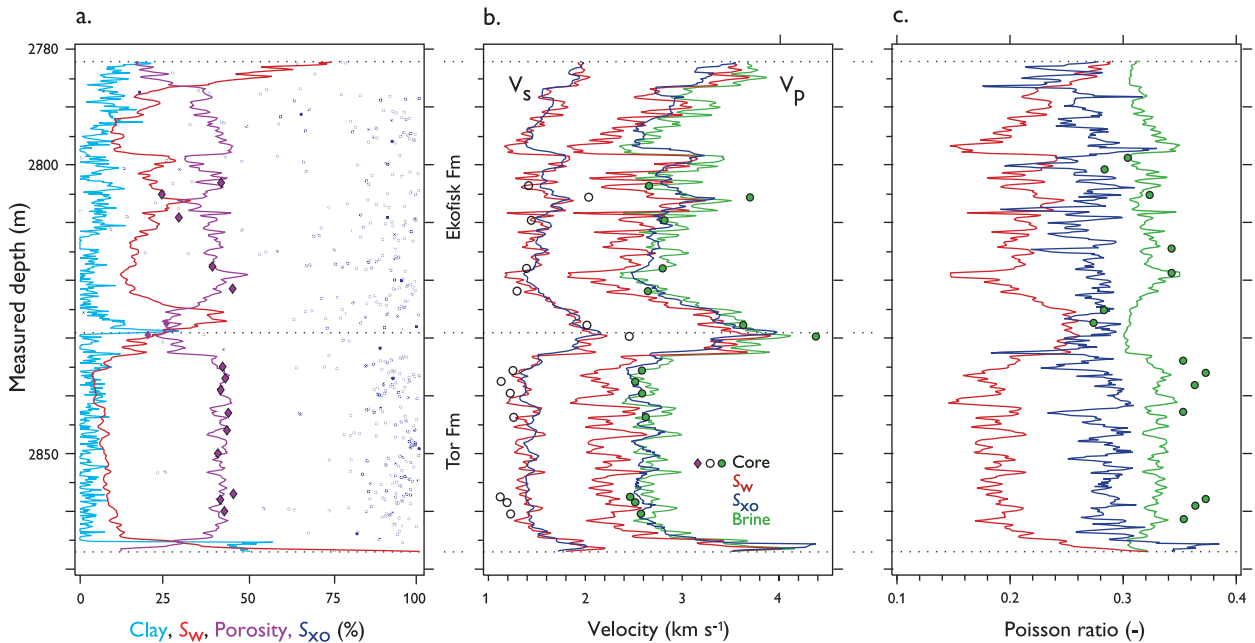


**Fig. 7.** Log data and predictions from the corrected MUHS model based on porosity and  $S_w$  for the chalk section in the Rigs-2 well (equations (2), (6); Figure 10). (a) Clay content (from gamma log), porosity and water saturation,  $S_w$  and  $S_{XO}$  (dots; equation (8)). (b) P- and S-velocity. Data and predictions of the corrected MUHS model. Brine-estimate for  $V_s$  not shown. (c) Poisson ratio. Data and predictions of the corrected MUHS model. In the high-porosity oil zone of the Tor Formation, the oil is predicted to be almost completely flushed as indicated by the closeness of the measured  $V_p(S_{XO})$  (blue curve) and the predicted  $V_p$ (brine) (green curve), whereas  $V_p$ (virgin zone,  $S_w$ ) is predicted to be low (cf. Figure 4).

#### Virgin zone properties estimated from the MUHS model

The acoustic properties of the virgin zone may be estimated from measured porosity and water saturation,  $S_w$ , in the virgin zone (Fig. 7):

1. Calculate the dry rock moduli from the MUHS model based on the porosity log (equation (2)).

2. Correct the moduli in the intervals with impure chalk, as estimated by  $S_w$ , by scaling the low-porosity end-member of the MUHS model (equation (6)).
3. Calculate the properties of the virgin zone with water saturation  $S_w$ , using Gassmann's relations and the Reuss mixing law (equations (A1), (A2)).

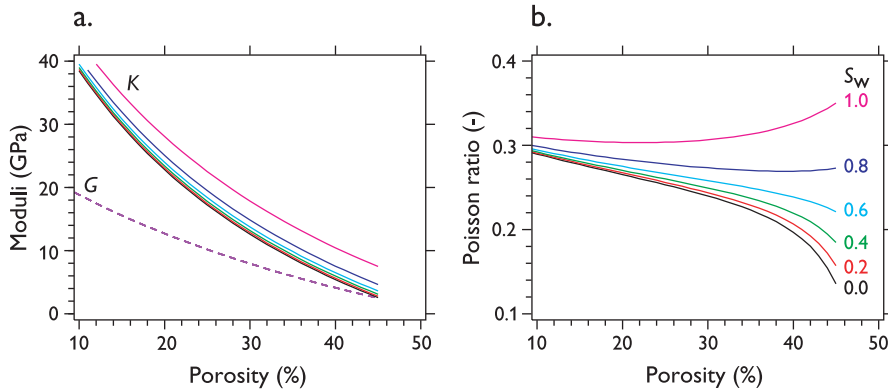


**Fig. 8.** Acoustic properties of chalk as a function of porosity and water saturation: (a) bulk and shear modulus; (b) Poisson ratio. Note the pronounced difference in Poisson ratio for porosities above  $\approx 30\%$  between brine and oil. MUHS prediction based on Reuss mixing and fluid properties for the South Arne Field (equations (2), (A2); Table 1).

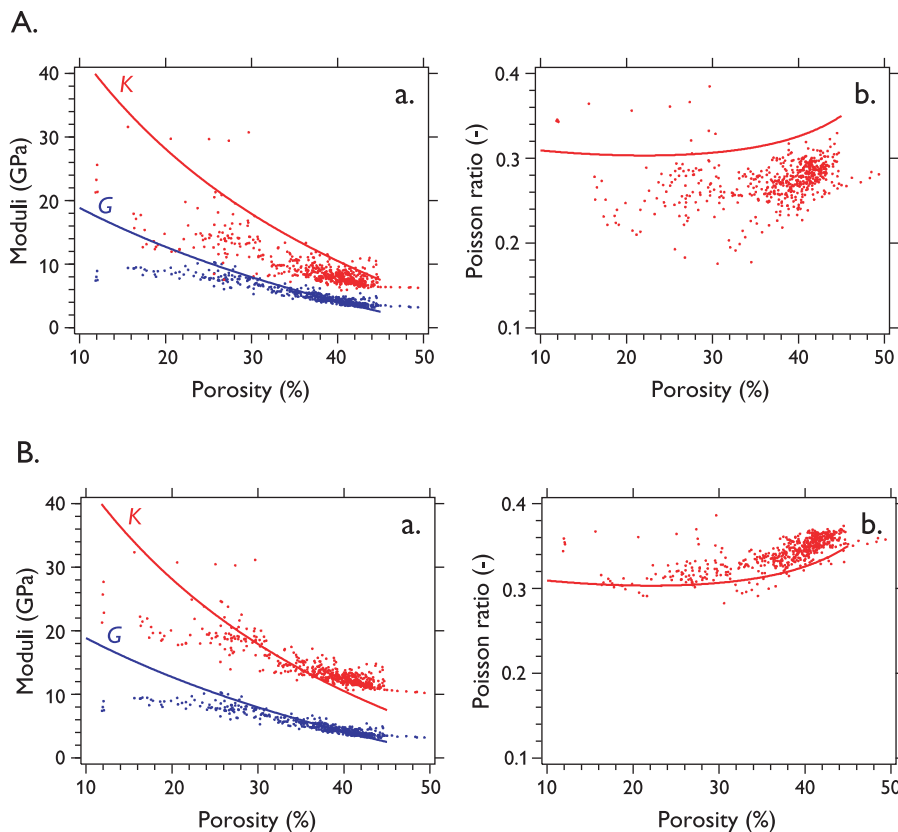


**Fig. 9.** Acoustic properties of log data for the chalk in the Rigs-2 well versus porosity. (A) Raw data. Bulk moduli plot below the MUHS model due to presence of hydrocarbons. (B) Substitution to brine conditions assuming no invasion. Bulk moduli plot above the MUHS model indicating that  $S_w$  overestimates the oil content near the wellbore. In both sets of diagrams, (a) shows bulk and shear modulus and (b) shows Poisson ratio. Note that the shear moduli – which are unaffected by fluid content – plot along the MUHS trend for  $\phi < 40\%$  and low  $S_w$  (pure chalk). Data points for low porosities below the trend line have high  $S_w$  and represent impure chalk. Full lines, MUHS model for chalk saturated with brine at reservoir conditions (equation (2); Table 1).

*MUHS model corrected for clay content.* Figure 10 shows the result of the uncorrected MUHS model (steps 1 and 3, dashed red curves) and the corrected MUHS model (steps 1 to 3, red curves) compared with the measured data (blue curves). The big difference in the bulk modulus between the model of the virgin zone and the data from the flushed zone is caused by removal of oil by mud invasion. However, the shear modulus is unaffected by fluid content and the model estimate of  $G$  is close to the data estimate. The difference in the estimates of the shear modulus is computed as  $\Delta G = G_{\text{MUHS}} - G_{\text{data}}$  for the uncorrected MUHS model, producing  $\Delta G$  up to 10 GPa where porosity is low (and moduli large) and where water saturation is high (Fig. 11). The clay content estimated from the gamma log reveals, however, no correlation with the mismatch between model and data. Furthermore,  $\Delta G$  is down to  $-2$  GPa for porosities above 40%, corresponding to the mismatch between log and core measurements of  $V_s$ , as discussed above. The interpretation of the relatively low S-velocities ( $\Delta G > 0$ ) measured at low porosities is that clay reduces porosity for a

given stiffness of the chalk matrix and, thus, moves the data point below the MUHS curve. The clay content estimated from the gamma log does not, however, correlate with  $\Delta G$ , probably because non-carbonate chalk constituents, such as quartz and smectite, have no or insignificant gamma response. Thus, water saturation is chosen as a measure of the clay content in the chalk. This is because the chalk is water-wet and the water saturation can be regarded as irreducible because it does not increase with depth (apart from the deepest 10 m of the Tor Formation). In this case, clay content and particle sorting become the controlling factor for the degree of water saturation in the chalk (cf. Fabricius *et al.* 2002).

In agreement with this conclusion, a clear distinction between the Ekofisk and the Tor formations is revealed by  $S_w$  but not by the gamma log (Fig. 7). The distinction between these formations is also evident from the well-known lower permeability of the Ekofisk Formation, which may be attributed to the higher content of silicates in the Ekofisk Formation (Røgen & Fabricius 2002). Low moduli for chalk

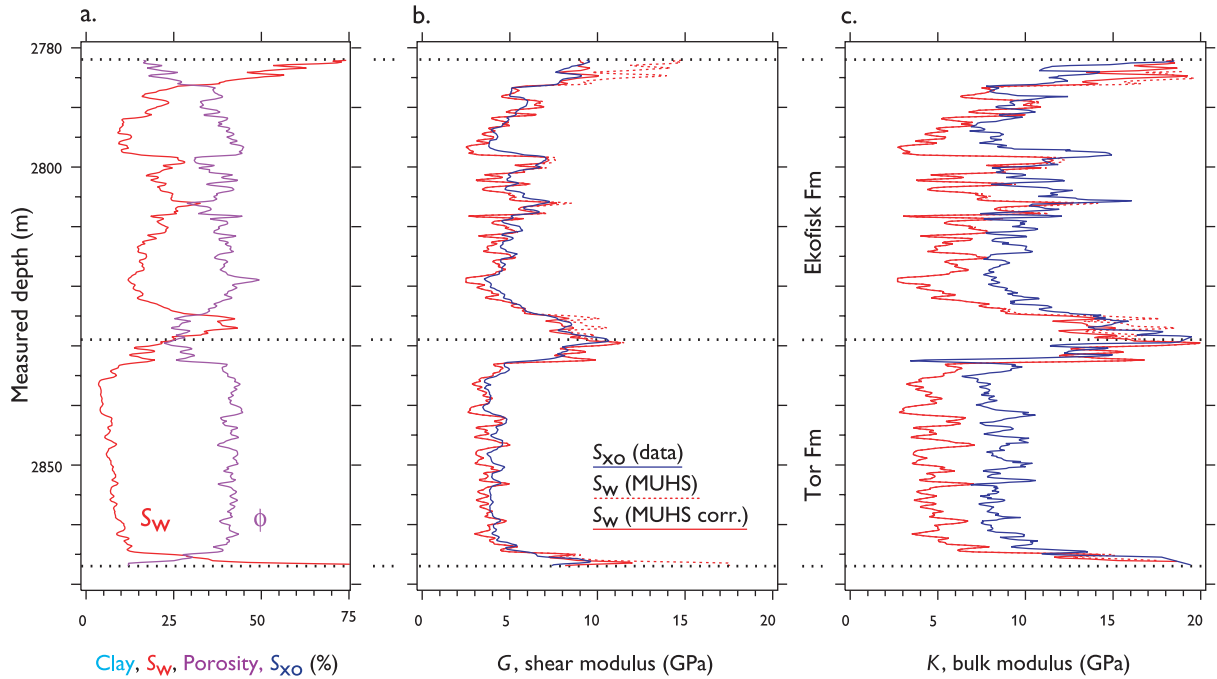


**Fig. 10.** Log response predicted for the virgin zone from the corrected and the uncorrected MUHS model compared with data from the invaded zone (equations (2), (6)). (a) Porosity and water saturation; (b) shear modulus; (c) bulk modulus. Note the good agreement between the shear modulus estimated from data and from the corrected MUHS model. Poor sorting and clay content may explain the difference between the estimated shear modulus from the uncorrected MUHS model and from the data in the tight zones (Figs 7, 11). The difference between the two estimates of the bulk modulus is caused by invasion of mud filtrate in the zone investigated by the sonic log.

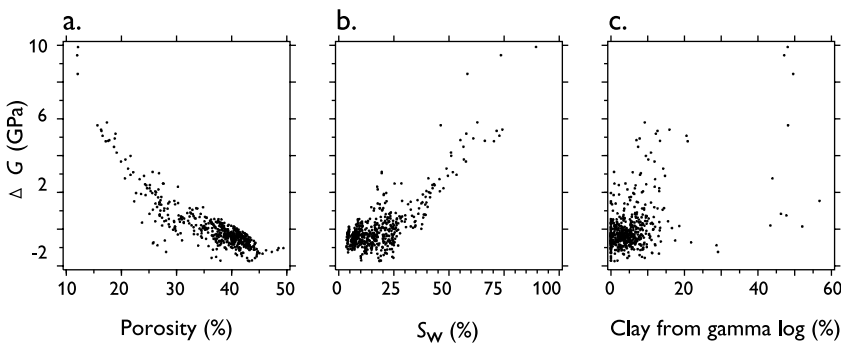


**Fig. 11.** Error in prediction of the shear modulus,  $\Delta G = \Delta G_{\text{MUHS}} - G_{\text{data}}$ , where  $G_{\text{MUHS}}$  is estimated from the MUHS model (equation (2)). (a)–(c).  $\Delta G$  versus porosity, water saturation and clay content estimated from the gamma log. The error in the MUHS model correlates with  $S_w$  and this indicates that the water saturation reflects the degree of impurity of the chalk in this reservoir where the chalk is water wet and the water saturation irreducible. The clay content estimated from the gamma log does not correlate with  $\Delta G$ .

with high shale content are also found for the plug data;  $\Delta G$  up to 10.5 GPa for 15% porosity (Fig. 2).

In order to correct the MUHS model (equation (2)) for the effect of clay, a simplistic, but apparently effective, approach has been chosen. The low-porosity end-member moduli,  $M_s$ , of the MUHS model has been scaled by the ‘clay’ content,  $c$ , taken as  $c = S_w - 0.2$ . For a given value of  $S_w$ ,  $M_s$  was calculated as a Hill average by computing the arithmetic average of the upper and lower Hashin–Shtrikman bounds,  $HS_U$  and  $HS_L$  (see Mavko *et al.* 1998):

$$M_s = (HS_U + HS_L)/2 \quad (6)$$

where the bounds are calculated as a mixture defined by  $c$  between the ‘no-clay’ end-member moduli for pure chalk given by Walls *et al.* (1998) –  $M_{\text{chalk}} = (65 \text{ GPa}, 27 \text{ GPa})$  – and the end-member moduli for pure clay given by Table 1 –  $M_{\text{clay}} = (25 \text{ GPa}, 9 \text{ GPa})$ . This procedure effectively scales  $M_s$  between  $M_{\text{chalk}}$  for  $S_w < 0.2$  and  $(30 \text{ GPa}, 11 \text{ GPa})$  for  $S_w = 1$ . The correction reduces the too high predictions of  $G$  to match

the data values in the low-porosity zones where  $S_w$  reaches maximum values (Fig. 10).

*Water saturation estimated from sonic data.* The bulk modulus,  $K_{\text{sat}}$ , of the flushed zone is known from the sonic data, whereas the dry-rock modulus,  $K_{\text{dry}}$ , of the chalk can be estimated from the corrected MUHS model (equation (6); Figure 10). One can now find the effective bulk modulus,  $k_{\text{fl}}$ , of the pore fluid in the flushed zone in terms of  $K_{\text{sat}}$  and  $K_{\text{dry}}$  by rearranging Gassmann’s relations (equation (A1)):

$$k_{\text{fl}} = \phi K_m \frac{A - B}{1 + \phi(A - B)}, \quad \text{where } A = \frac{K_{\text{sat}}}{K_m - K_{\text{sat}}}, B = \frac{K_{\text{dry}}}{K_m - K_{\text{dry}}} \quad (7)$$

Substituting this result into the Reuss equation for fine-scaled fluid mixing (equation (A2)), produces the saturation of the flushed zone,  $S_{\text{xo}}$ :

$$S_{\text{xo}} = \frac{k_{\text{brine}}(k_{\text{oil}} - k_{\text{fl}})}{k_{\text{fl}}(k_{\text{oil}} - k_{\text{brine}})} \quad (8)$$

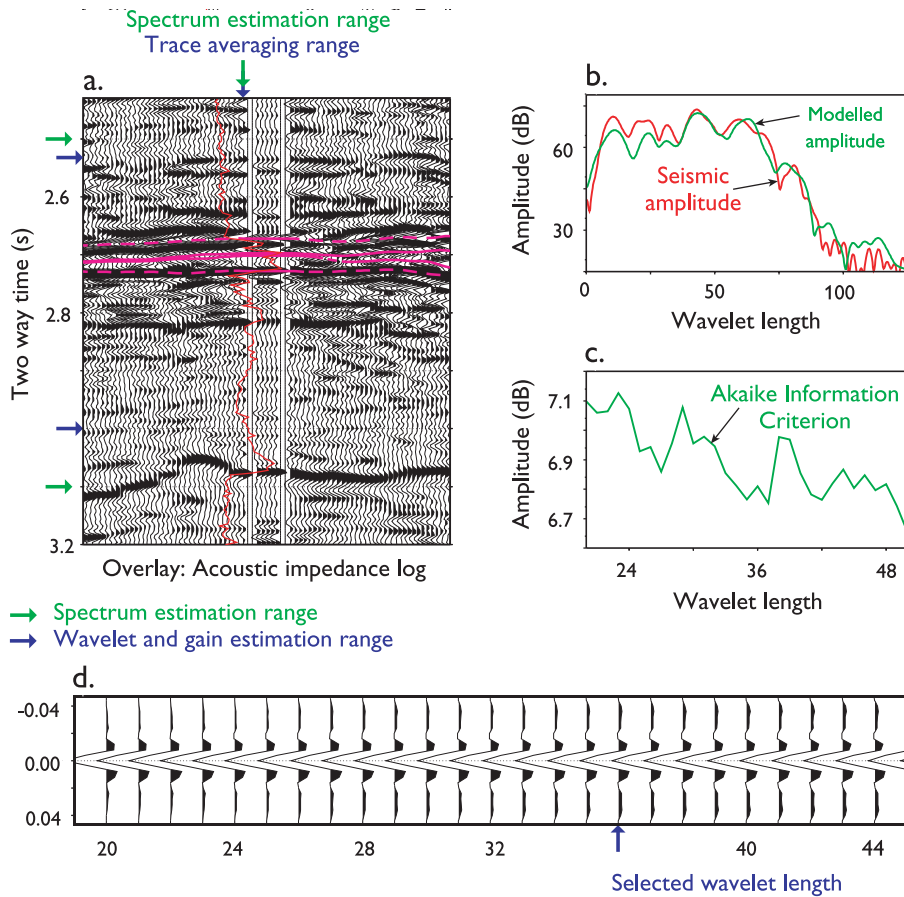


**Fig. 12.** Near-offset stack; least-squares wavelet estimation in well I-1x. (a) Synthetic seismic trace obtained by convolution of the optimum wavelet (length 36 samples) with the near-offset angle reflectivity log from the well inserted into the seismic data. (b) Amplitude spectra in the wavelet estimation window of the seismic trace at the well location and the synthetic seismic trace. (c) Akaike's misfit criterion (Akaike 1981). (d) Wavelet suite. The lengths of the predicted wavelets range from 20 samples to 44 samples (80 ms to 176 ms, horizontal axis).

where  $k_{oil}$  and  $k_{brine}$  are the bulk moduli of oil and brine in the reservoir (Table 1). Only values of  $S_{xo}$  between 0 and 1 are valid (234 out of 306 data points).  $S_{xo}$  has a large scatter and values above 90% are found for much of the Tor reservoir where porosity exceeds 40% (Fig. 7).

**Resulting acoustic response.** The acoustic properties of the invaded zone can now be estimated by the velocity logs (blue curves in Figure 7) and the water saturation  $S_{xo}$  estimated by equation (8). The properties of the virgin zone (red curves) are found from the corrected MUHS model based on porosity and  $S_w$ . A significant difference in  $V_p$  is predicted between the virgin zone and the invaded zone, but not between the invaded zone and the prediction for pure brine (green curve) because of the almost complete mud filtrate invasion.

#### AVO INVERSION BASED ON LOGS FROM THE MUHS MODEL

AVO attributes were calculated from inverted 2D seismic lines (near- and far-offset data) extracted from the South Arne 3D survey. The inversion was carried out for the two-way time window 1.9–3.6 s and was targeted on the chalk interval (cf. Cooke & Schneider 2003). Log data from the I-1x, Rigs-1, -2 and SA-1 wells were used in the inversion process. These data comprise  $V_p$ - and  $V_s$ -data, based on the corrected MUHS model described above, plus density logs, check shot and deviation data. Wavelets were estimated for each offset stack using a least-squares wavelet estimation method with constraints on the phase. Wavelet estimations were carried out for each of the wells (Fig. 12). Since the I-1x well has no shear log data,  $V_p/V_s=2$  was used in the calculations. The wavelet estimated from the I-1x well was preferred based on inversion tests.

Low-frequency components of the acoustic impedance variations with depth are not present in seismic data. Since this information is essential to the interpretation, it should be accounted for in the seismic inversion. Low-frequency near- and far-angle impedance models were constructed by extrapolating the angle-dependent impedance well logs through the 3D volume tied to seismic horizons, followed by low-pass filtering (cf. Castagna & Backus 1993). The final inversion models 93.7% of the seismic energy for the near-offset stack and 93.4% for the far-offset stack. The inversion results are good in terms of match with the angle impedance well logs.

AVO attributes were computed from the angle-dependent impedance inversions combined with low-frequency information (Bach *et al.* 2003). Acoustic impedance, shear impedance and Poisson's ratio were extracted at the location of the Rigs-2 well. The AVO results are good in terms of match with the well log data. Low values of Poisson's ratio at the location of Rigs-2 are in agreement with the presence of light oil in the high-porous chalk of the South Arne Field (Fig. 13).

#### DISCUSSION

The plot of Poisson's ratio versus depth in Figure 7 reveals a characteristic pattern with pronounced peaks at top Ekofisk and top Tor and low values in the highly porous Tor reservoir. This pattern is in good agreement with the inverted seismic data (Fig. 13) and results from forward modelling of the acoustic properties of the virgin zone, but these features are not captured in the approach based on Land's (1968) equation (Fig. 6).

It is, therefore, suggested that Land's equation underestimates the mud-invasion close to the wellbore in the porous part of the reservoir and that the shallow resistivity log also reflects

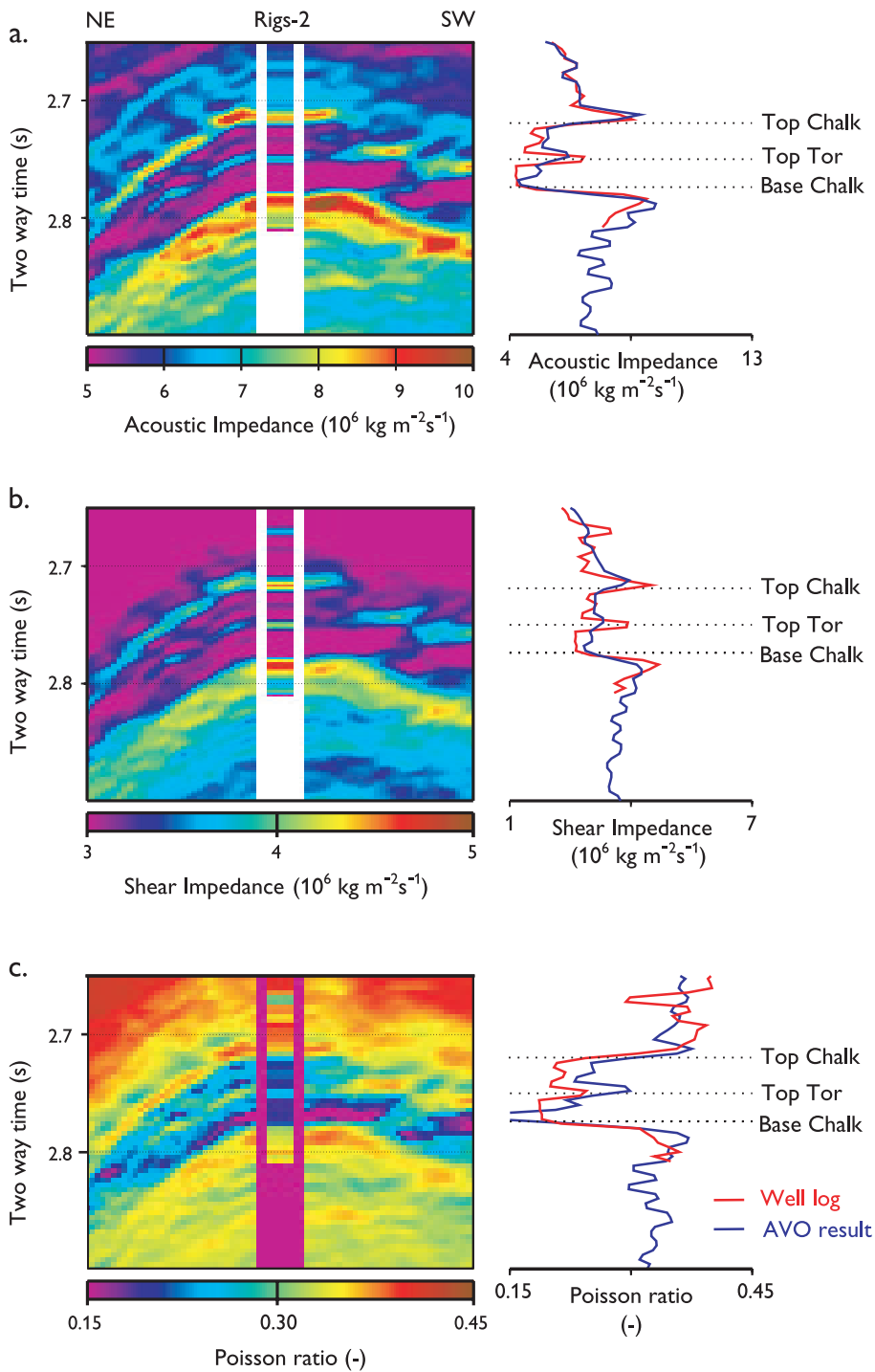


**Fig. 13.** Two-way time section with AVO inversion of seismic data and inserted log response for the Rigs-2 well computed from forward modelling of the corrected MUHS model (Fig. 7). (a) Acoustic impedance; (b) shear impedance; (c) Poisson ratio. Very good agreement is observed for both acoustic and shear impedance. Note the peaks in the tight zones near top chalk and top Tor. There is good agreement between the log- and AVO-pattern of Poisson's ratio, e.g. the peak at top Tor and the low values within the Tor Formation. This pattern cannot be resolved by the log if the acoustic properties are estimated from the sonic log because the water saturation near the wellbore is unknown (Fig. 6).

the conditions at some distance from where the P-waves are propagated. This suggestion is further supported by two observations. First, that the sonic velocity recorded by the logging tool is close to the ultrasonic velocity measured on core samples saturated with brine (Fig. 5b). Secondly, that the porosities estimated from the bulk density match core porosities if full invasion of mud filtrate is assumed to have taken place (Fig. 3).

The content of hydrocarbons, thus, appears to drop to a very low value close to the wellbore where the  $V_p$  reaches its maximum value, thereby restricting the propagation of P-waves to a very narrow zone, whereas the S-waves are much less sensitive to the fluid content and, consequently, are propagated over a wider zone.

Land's equation may describe mud invasion under spontaneous imbibition conditions equivalent to a reduction of capillary pressure to zero. However, in the immediate vicinity of the borehole, mud pressures may become so high that capillary pressures drop below zero causing forced displacement of non-wetting fluids. This causes oil saturation to go below that predicted by the Land equation as has also been shown by Spinler *et al.* (2002).

The best way to estimate the acoustic properties of the virgin zone is to use the extended modified upper Hashin-Shtrikman velocity–porosity relation for chalk presented here. AVO inversion of the seismic data based on such synthetic sonic logs reveals a zone of very low Poisson's ratio that correlates with the oil reservoir in the Tor Formation. AVO

inversion, thus, provides direct evidence for the presence of oil in high-porous chalk saturated with the light oil of the South Arne Field.

## CONCLUSIONS

The modified upper Hashin–Shtrikman trend established by Walls *et al.* (1998) has been extended for chalk on the Ekofisk Field by using ultrasonic data from high-porosity chalk samples from the South Arne Field. Calculation of the acoustic properties of chalk as a function of water saturation, based on this model and Gassmann's relations, predict a pronounced drop in Poisson's ratio for oil-bearing chalk with porosities above  $\epsilon$  30%.

Shaley chalk samples have significantly smaller P- and S-velocities and a higher Poisson's ratio than the general data trend. The relative drop in velocities are probably due to the reduction in porosity caused by smectite, which does not affect the stiffness of the sediments. The shear moduli estimated from log data are increasingly smaller the MUHS model at lower porosities and this deviation correlates with increasing water saturation, but not with clay content estimated from the gamma log. This deviation is interpreted to be due to the clay content that controls the water saturation in the zone of irreducible water saturation in water-wet chalk.

Comparison of estimates of  $V_p$  and porosity from log and core data clearly shows that the logging data records the conditions of a zone close to the wellbore where mud filtrate has almost completely flushed the reservoir. Estimating invasion effects is usually difficult because of the lack of different types of data, but this study underlines the importance of having access to core data. Comparison of estimates of  $V_s$  shows that the core data record a smaller velocity than the log data for low velocities and this could be due to S-waves finding a 'fast path' some distance from the wellbore, whereas the P-waves are restricted to a narrow zone where  $V_p$  and  $S_w$  have maximum values.

The best way to estimate the acoustic properties of the reservoir is to use the MUHS model presented here, with porosity and water saturation of the virgin zone as input. AVO inversion of the seismic data based on such synthetic sonic logs reveals a zone of very low Poisson's ratio that correlates with the oil reservoir in the Tor Formation. AVO inversion, thus, provides direct evidence for presence of oil in high-porous chalk saturated with the light oil of the South Arne Field.

These results are part of the outcome of the energy research project Rock Physics of Impure Chalk which was sponsored by the Danish Energy Research Program (EFP-2001), Amerada Hess A/S and Dong E&P. Lars Gommessen contributed to many discussions and James Chalmers helped correct the English. The authors thank referees P. Dromgoole, R. Simm and J. Gallagher for constructive critiques. The authors would like to honour the memory of Jacob Mørch Pedersen who died recently: he was a source of great inspiration in our common work.

## APPENDIX A: Rock physics relations

### A.1: Fluid substitution using Gassmann's equations

The bulk and the shear moduli,  $K$  and  $G$  [GPa], of a rock are computed from  $V_p$ ,  $V_s$  [ $\text{km s}^{-1}$ ] and density [ $\text{g cm}^{-3}$ ]:  $K = \rho(V_p^2 - 4/3 \cdot V_s^2)$ ,  $G = \rho V_s^2$ . The moduli of the rock for the initial fluid saturation (fluid 1) can be transformed to moduli of the rock saturated with a new fluid (fluid 2) using Gassmann's (1951) relations (see Mavko *et al.* 1998):

$$K_{\text{sat}2} = K_m \cdot A / (1 + A), G_{\text{sat}1} = G_{\text{sat}2} \text{ where} \\ A = \frac{K_{\text{sat}1}}{(K_m - K_{\text{sat}1})} - \frac{K_{\text{fl}1}}{\phi(K_m - K_{\text{fl}1})} + \frac{K_{\text{fl}2}}{\phi(K_m - K_{\text{fl}2})} \quad (\text{A1})$$

$K_{\text{sat}1}$ ,  $K_{\text{sat}2}$  are the bulk modulus of rock with the original and new pore fluid;  $K_m$  is the bulk modulus of mineral material making up rock;  $K_{\text{fl}1}$ ,  $K_{\text{fl}2}$  are the bulk modulus of the original and the new pore fluid;  $G_{\text{sat}1}$ ,  $G_{\text{sat}2}$  are the shear modulus of rock with the original and the new pore fluid. The shear modulus is predicted to be unaffected by fluid content. Gassmann's equations are established for homogeneous mineral modulus and statistical isotropy and are valid at sufficiently low frequencies that the pore pressures induced by the sonic wave are equilibrated throughout the pore space. Gommessen *et al.* (2002) found that Gassmann's theory may be applied to chalk at logging frequencies and this was further supported by analysis of ultrasonic velocities on chalk samples (Japsen *et al.* 2002). Therefore, Gassmann's relations are applied to calculate the effects on the acoustic properties of chalk estimated from logging data when one pore fluid is substituted by another.

### A.2: Properties of mixed fluids

The exact bulk modulus,  $K_{\text{fl}}$ , of mixtures of fluids with moduli,  $K_{\text{fl}1}$  and  $K_{\text{fl}2}$  can be calculated as a Reuss average ('lower bound') if the fluids form a homogeneous mixture (Fig. 4; see Mavko *et al.* 1998):

$$1/K_{\text{fl}} = S_{\text{fl}1}/K_{\text{fl}1} + (1 - S_{\text{fl}1})/K_{\text{fl}2} \quad (\text{A2})$$

where  $S_{\text{fl}1}$  is the relative saturation of fluid 1 (e.g. brine,  $S_w$ ). Even small amounts of the light component (e.g. hydrocarbon or air) reduce the bulk modulus of the mixed fluid significantly because the average modulus is calculated from the inverse values of the individual moduli.

The properties of mixtures can be estimated as a Voigt average as an approximation to the patchy saturation 'upper bound' where the fluids are not evenly distributed:

$$K_{\text{fl}} = S_{\text{fl}1} \cdot K_{\text{fl}1} + (1 - S_{\text{fl}1}) \cdot K_{\text{fl}2} \quad (\text{A3})$$

Here, the average modulus is more dependent on the denser constituents. Reuss mixing is assumed to be the best approximation at logging frequencies in chalk because Reuss mixing appears to be dominant even at ultrasonic frequencies (see the 'Results' section).

### A.3: Modified upper Hashin–Shtrikman (MUHS) model

Walls *et al.* (1998) found that a modified upper Hashin–Shtrikman (MUHS) model predicts the velocity–porosity behaviour of chalk as estimated from well log data from the Ekofisk Field (porosities from 10% to 40%). The model describes how the dry bulk and shear moduli,  $K$  and  $G$ , increase as porosity is reduced from a maximum value,  $f\phi_{\text{max}}$ , to zero porosity. The upper and lower Hashin–Shtrikman bounds give the narrowest possible range on the modulus of a mixture of grains and pores without specifying the geometries of the constituents (Hashin & Shtrikman 1963). The upper bound represents the stiffest possible pore shapes for porosity ranging from 0% to 100%, whereas the modified upper bound is defined for porosity up to a maximum value less than 100%. Here, the high-porosity end-member is referred to as the maximum porosity rather than as the critical porosity, which is defined as the porosity limit above which a sedimentary rock can only exist as a suspension (Nur *et al.* 1998). The low-

porosity end-members,  $K_s$  and  $G_s$ , are the moduli of the solid at zero porosity found by extrapolation of the data trend. The modified upper Hashin–Shtrikman model is given by the dry-rock bulk and shear modulus,  $K^{\text{MUHS}}$  and  $G^{\text{MUHS}}$ :

$$K^{\text{MUHS}} = \left[ \frac{\varphi/\varphi_{\text{max}}}{K_{\varphi_{\text{max}}} + \frac{4}{3}G_s} + \frac{1 - \varphi/\varphi_{\text{max}}}{K_s + \frac{4}{3}G_s} \right]^{-1} - \frac{4}{3}G_s$$

$$G^{\text{MUHS}} = \left[ \frac{\varphi/\varphi_{\text{max}}}{G_{\varphi_{\text{max}}} + Z_s} + \frac{1 - \varphi/\varphi_{\text{max}}}{G_s + Z_s} \right]^{-1} - Z_s, \quad (\text{A4})$$

$$\text{where } Z_s = \frac{G_s \cdot 9K_s + 8G_s}{6 \cdot K_s + 2G_s}$$

The end-member moduli of the dry rock found by Walls *et al.* (1998) for chalk on the Ekofisk Field based on log data were

$$K_{\varphi_{\text{max}}} = 4 \text{ GPa}, G_{\varphi_{\text{max}}} = 4 \text{ GPa for } \varphi_{\text{max}} = 40\%, \text{ and}$$

$$K_s = 65 \text{ GPa}, G_s = 27 \text{ GPa for } \varphi = 0\% \quad (\text{A5})$$

From this model one can calculate the moduli of the dry rock for a given porosity and then estimate the moduli for the saturated rock using Gassmann's relations (equation (A1)) and the appropriate fluid properties (using equation (A2)) at logging frequencies) and finally calculate  $V_p$  and  $V_s$ .

## REFERENCES

- Akaike, H. 1981. Modern development of statistical methods. In: Eykhoff, P. (ed.) *Trends and progress in system identification*. Pergamon Press, Elmsford, NY, 169–184.
- Bach, T., Espersen, T.B., Pedersen, J.M., Rasmussen, K.B., Hinkley, R. & Pillet, R.P. 2000. Seismic inversion of AVO data. In: Hansen, P.C., Jacobsen, B.H. & Mosegaard, K. (eds) *Methods and Applications of Inversion*. Springer Verlag, Berlin, 31–42.
- Castagna, J.P. & Backus, M.M. 1993. *Offset-dependent reflectivity – Theory and practice of AVO analysis*. Society of Exploration Geophysicists, Tulsa.
- Cooke, D.A. & Schneider, W.A. 2003. Generalised linear inversion of reflection seismic data. *Geophysics*, **48**, 665–676.
- Engström, F. 1995. A new method to normalise capillary pressure curves. Paper presented at the International Symposium of the Society of Core Analysis.
- Fabricius, I.L. 2003. How burial diagenesis of chalk sediments controls sonic velocity and porosity. *American Association of Petroleum Geologists Bulletin*, **87**, 1755–1778.
- Fabricius, I.L., Mavko, G., Mogensen, C. & Japsen, P. 2002. Elastic moduli of chalk as a reflection of porosity, sorting, and irreducible water saturation. *72nd SEG Annual Meeting, Salt Lake City, USA, proceedings*, 1903–1906.
- Gassmann, F. 1951. Elastic waves through a packing of spheres. *Geophysics*, **16**, 673–685.
- Gommesen, L. 2003. *Prediction of porosity and fluid in chalk from acoustic measurements*. PhD thesis. Technical University of Denmark (DTU).
- Gommesen, L., Mavko, G., Mukerji, T. & Fabricius, I.L. 2002. Fluid substitution studies for North Sea chalk logging data. *72nd SEG Annual Meeting, Salt Lake City, USA, proceedings*, 4pp.
- Hashin, Z. & Shtrikman, S. 1963. A variational approach to the elastic behaviour of multiphase materials. *Journal of the mechanics and physics of solids*, **11**, 127–140.
- Jacobsen, N.L., Engström, F., Uldall, A. & Petersen, N.W. 1999. Delineation of hydrodynamic/geodynamic trapped oil in low permeability chalk. Paper SPE56514, presented at the SPE Annual Technical Conference.
- Japsen, P. 1998. Regional velocity–depth anomalies, North Sea Chalk: a record of overpressure and Neogene uplift and erosion. *American Association of Petroleum Geologists Bulletin*, **82**, 2031–2074.
- Japsen, P., Wagner, H., Gommesen, L. & Mavko, G. 2000. Rock physics of Chalk: modelling the sonic velocity of the Tor Formation, Danish North Sea. Paper presented at the EAGE 62nd Annual Conference and Technical Exhibition, Glasgow, Scotland, 4pp.
- Japsen, P., Høier, C., Rasmussen, K.B., Fabricius, I.L., Mavko, G. & Pedersen, J.M. 2002. Effect of fluid substitution on ultrasonic velocities in chalk plugs, South Arne field, North Sea. *72nd SEG Annual Meeting, Salt Lake City, USA, proceedings*, 1181–1184.
- Land, C.S. 1968. Calculation of imbibition relative permeability for two- and three-phase flow from rock properties. *Society of Petroleum Engineers Journal*, **1968**, 149–156.
- Mackertich, D.S. & Goulding, D.R.G. 1999. Exploration and appraisal of the South Arne Field, Danish North Sea. In: Fleet, A.J. & Boldy, S.A.R. (eds) *Petroleum Geology of Northwest Europe: Proceedings of the 5th Conference*. Geological Society, London, 959–974.
- Mavko, G., Mukerji, T. & Dvorkin, J. 1998. *The rock physics handbook*. Cambridge University Press, Cambridge.
- Megson, J.B. 1992. The North Sea chalk play; examples from the Danish Central Graben. In: Hardman, R.F.P. (ed.) *Exploration Britain: Geological insights for the next decade*. Geological Society, London, Special Publications, **67**, 225–247.
- Nur, A., Mavko, G., Dvorkin, J. & Galmundi, D. 1998. Critical porosity; a key to relating physical properties to porosity in rocks. *Leading Edge*, **17**, 357–362.
- Røgen, B. 2002. *North Sea chalk – textural, petrophysical and acoustic properties*. PhD thesis. Technical University of Denmark (DTU).
- Røgen, B. & Fabricius, I.L. 2002. Influence of clay and silica on permeability and capillary entry pressure of chalk reservoirs in the North Sea. *Petroleum Geoscience*, **8**, 287–293.
- Røgen, B., Fabricius, I.L., Japsen, P., Høier, C., Mavko, G. & Pedersen, J.M. In press. Ultrasonic velocities of chalk samples – influence of porosity, fluid content and texture. *Geophysical Prospecting*.
- Scholle, P. 1977. Chalk diagenesis and its relation to petroleum exploration; oil from chalks, a modern miracle? *American Association of Petroleum Geologists Bulletin*, **61**, 982–1009.
- Spinler, E.A., Baldwin, B.A. & Graue, A. 2002. Experimental artefacts caused by wettability variations in chalk. *Journal of Petroleum Science and Engineering*, **33**, 49–59.
- Vejbæk, O.V. & Kristensen, L. 2000. Downflank hydrocarbon potential identified using seismic inversion and geostatistics: Upper Maastrichtian reservoir unit, Dan Field, Danish Central Graben. *Petroleum Geoscience*, **6**, 1–13.
- Vejbæk, O.V., Rasmussen, R., Japsen, P., Bruun, A., Pedersen, J.M., Marsden, G. & Fabricius, I.L. 2005. Modelling seismic response from North Sea Chalk reservoirs resulting from changes in burial depth and fluid saturation. In: Doré, A.G. & Vining, B. (eds) *Petroleum Geology - NW Europe and Global Perspectives: Proceedings of the 6th Conference*. Geological Society, London, 1401–1414.
- Walls, J.D., Dvorkin, J. & Smith, B.A. 1998. Modeling seismic velocity in Ekofisk Chalk. *68th SEG Annual Conference*, 1016–1019.